京都大学防災研究所年報 第 49 号 B 平成 18 年 4 月
Annuals of Disas. Prev. Res. Inst., Kyoto Univ., No. 49 B, 2006

Dynamic Behavior of a Levee on Saturated Sand Deposit

Tetsuo TOBITA, Susumu IAI, Kyohei UEDA*

* Department of Civil and Earth Resource Engineering, Kyoto University

Synopsis

Dynamic behavior of an embankment (3 m height) made of dry sand underlain by saturated sand deposit with 5 m depth are studied. Firstly, centrifuge experiments under 50 G are conducted. The relative density of saturated sand deposit is approximately either 30 % or 70 %. Sinusoidal input motions with various levels of peak acceleration amplitude are employed. Test results show that the maximum settlement was 1.4 m and 0.09 m, respectively, for loose and dense deposit. The amount of settlements for dense deposit are found to be proportional to the peak amplitude of input acceleration, while it may have a plateau for the case of loose deposit with increase of input acceleration amplitude. Following the centrifuge experiments, an effective stress analysis is carried out with the same prototype dimension of the experiments. The numerical analysis simulates well deformations and transient motions of the experimental counterparts. It is found that, in the analysis for loose deposit, when input acceleration increased, non-liquefied area underneath the embankment became large, causing larger non-liquefied wedge pushing liquefied soils aside.

Keywords: Levee, dynamic behavior, liquefaction, centrifuge experiment, numerical analysis

1. Introduction

Liquefaction have caused tremendous damage to earth structures, such as, earth dams, embankments and river dikes (Bardet and Davis 1996, Seed et al. 1975, Seed et al. 1990). After the 1995 Hyogo-ken Nanbu, Japan, earthquake, for example, river dikes along the Yodo river with total length of about 9.3 km were severely damaged due to liquefaction (Matsuo 1996). After the 2003 Tokachi-oki, Japan, earthquake, river dikes were damaged at 66 locations with total length of about 27 km (Nishimoto 2003). Not only the failure of structures themselves, but also second disaster, such as inundation or flooding, may occur after their collapses [e.g., the 1948 Fukui, Japan, earthquake (GHQ-Report 1948)]. Triggered by those devastating damage after large earthquakes, dynamic behavior of an embankment have been studied experimentally and numerically by many researchers. Extensive literature review can be found in Adalier et al. (1998).

Experimental studies have been conducted using the shaking table in 1G field, [e.g. Koga and Matsuo (1990)] or centrifuge field [e.g., Adalier et al. (1998); Adalier and Sharp (2004); Fiegel and Kutter (1994); Koseki et al. (1994)] Takeuchi et al. (1991) conducted shaking table tests on dikes founded on saturated sand deposit and investigated the effectiveness of compaction as a countermeasure against flow-type of deformation. In a series of tests they conducted, when the area of compaction is in the free field near the toe, compacted area did not move but the dike deformed excessively, while the area of compaction is beneath the dike, the compacted area acted effectively and the deformations were very small.

Kazama et al. (1996) conducted centrifuge testing for an embankment made of sands with two different centrifugal accelerations and verified the applicability of

similitude law. They also carried out stability analysis with the Swedish method by taking account of the effects of acceleration and pore water pressure buildup and suggested possibility of the static analysis to the stability of embankments resting on liquefiable sand deposit.

Major difficulty associated with computation of flow-liquefaction arises when the dynamic behavior of embankments on saturated sand deposit is considered. Yasuda et al. (1999) proposed a static FE method to evaluate the amount of liquefaction-induced flow by using bilinear stress-strain relationship calibrated against data obtained from the combination of cyclic and static loading tests. Their model utilizes the stress-strain curve constituted of low rigidity region and rigidity recovering region as strain being large, and simulates well deformations of structures associated liquefaction-induced flow.

When earth structures were designed or remediation measures are practiced based on displacement criteria which is much cost effective than those based on the factor of safety approach [Finn (2000); ISO23469 (2005)], it is required to specify and verify the criteria for serviceability and safety. Those criteria for embankments may be given by the amount of crest settlements against intensity of input motion. Therefore, the development of methodology to check if a designed structure behaves within those criteria is of prime importance. Thus, the objective of the present study is to verify the applicability of the effective stress analysis proposed by Iai et al. (1992) by comparing results with experimental counterparts. In what follows, units are in prototype, if not otherwise specified.

2. Centrifuge experiments

Experiments were carried out in a rigid wall container mounted on the 2.5 m radius geotechnical centrifuge at the Disaster Prevention Research Institute, Kyoto University (DPRI-KU). Overall dimension of the rigid container is 450 x 150 x 300 mm in length, width, and height, respectively (Fig. 1). Dynamic excitation was given in

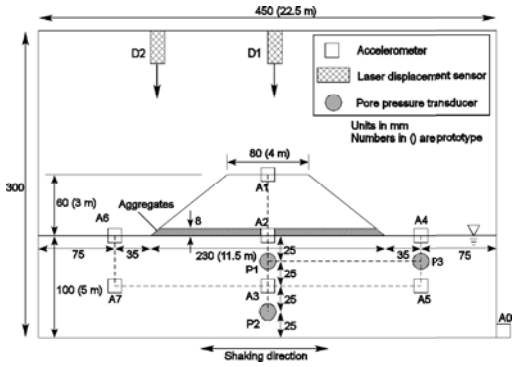

Fig. 1. Model configuration in rigid container.

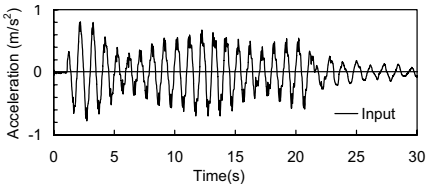

Fig. 2. Input acceleration for Case 1.

Table 1. Summary of test cases

Case	Soil type	Dr (%)	Max. input acceleration	Settlements (m)
1		27	81	0.01
2	Loose	30	179	1.00
3		30	313	1.40
4		69	79	0.00
5	Dense	71	169	0.01
6		67	574	0.09

Table 2. Model parameters for deformation properties.

Soil Type	Corrected SPT Blow count, N	Density	Porosity	Parameter for deformation characteristic							
				Elastic tangent shear modulus at p_r	Elastic tangent bulk modulus at p_r	Reference mean effectve stress	Poisson ratio	Exponent of a power function for modulus	Internal friction angle	Cohesion	Max. damping ratio
		ρ	n	G_r	K_r	p_r	v	m	φ_f	c	h_{max}
	(N_{65})	(kg/m^3)		(kPa)	(kPa)	(kPa)			(°)	(kPa)	
Loose	1	1.34×10^3	0.498	1.987×10^4	5.182×10^4				37.50		
Dense	40	1.45×10^3	0.451	1.885×10^5	4.916×10^5	98.0	0.33	0.50	43.27	0.0	0.24
Levee	40	1.45×10^3	0.450	1.885×10^5	4.916×10^5				43.27		

Table 3. Model parameters for liquefaction properties.

Soil Type	Corrected SPT blow count, (N_{65})	Parameter for liquefaction characteristic					
		Phase trans. Ang.	Parameters for dilatancy				
		φ_p (°)	w_1	p_1	p_2	c_1	S_1
Loose	5	28.0	4.634	0.50	1.037	1.548	0.005
Dense	40	28.0	21.40	0.50	0.407	13.26	0.005

longitudinal direction. The applied centrifugal acceleration was 50 G. A shake table unidirectionally driven by a servo hydraulic actuator is mounted on a platform and it is controlled through a laptop computer on the centrifuge arm. All the equipment necessary for shake table control is put together on the arm. The laptop PC is accessible during flight from a PC in the control room through wireless LAN and "Remote Desktop Environment" of WindowsXP (Microsoft 2003).

A model configuration shown in Fig. 1 is a cross section of an embankment resting on a saturated sand deposit. The crest height is 3.0 m, and lateral length at the top and bottom are, respectively, 4.0 m and 11.5 m. and side slope of 1:1.25. The model was instrumented with 8 accelerometers (SSK, A6H-50), 2 laser displacement transducers (Keyence, LB-080) and 3 pore water pressure transducers (SSK, P306A-5) (Fig. 1). All the electric data was recorded by digital data recorders (TML, DC-104R) mounted on the centrifuge arm. Sampling frequency was 5 kHz.

Silica sand ("Soma" sand No. 5) (e_{max}=1.11, e_{min} = 0.69, D50 = 0.38 mm) were used for both the deposit and embankment. Only the sand deposit was saturated with viscous fluid (Metolose, SM-25 Shin-Etsu Chemical Co.) whose viscosity was adjusted to 50 times of water (50 cSt).

Total six tests were employed as shown in Table 1. Two types of sand deposit were prepared by water-pluviating sand to relative densities of approximately 30 % and 70 % for, respectively, loose and dense deposit in about 100 mm lifts (model scale). Before filling sands, rehydratable noodles, which served as inclinometers for saturated sand deposit, were attached to the inner side of Plexiglas-like wall installed in the soil container. The embankment was made by dry sand with the relative density approximately 70 %. Aggregates were placed at the bottom of the embankment aiming at preventing the embankment from soaking up pore water by suction.

Input motion was intended to be sinusoidal with 1 Hz and 20 waves. However, as shown in Fig. 2, for example, the amplitude was not constant. This might be due to the effect of mechanical resonance with the centrifuge arm during shaking. In a series of the experiments, the peak amplitude of input acceleration was varied (Table 1) to see their effects on deformation characteristics of an embankment.

3. Numerical analysis by FLIP

To see the applicability of the effective stress analysis by FLIP (Iai et al. 1992), results of the numerical analysis are compared with the experimental counterparts. The numerical model dimension was set as the prototype scale. The analysis constituted of four steps of self-weight analysis under drained condition as indicated by STEP1 to STEP4 in Fig. 3, and a dynamic analysis under undrained condition. The recorded input motion was specified along the base. For solid phase, to mimic boundary conditions of the rigid container, displacement degrees of freedom at the base were fixed both horizontally and vertically, and at two lateral boundaries, only lateral displacements were fixed. For liquid phase, zero pressure was prescribed at the surface of the deposit and at the bottom of the embankment

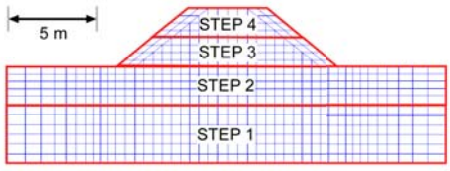

Fig. 3. Finite element mesh for numerical analysis. The areas indicated by STEPs are order of self-weight analysis.

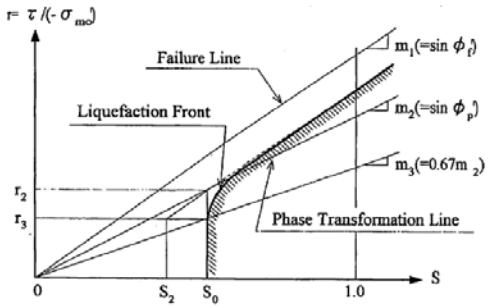

Fig. 4. Schematic view of the pore pressure model implemented in FLIP (Iai et al. 1992)

(water table is precisely at the surface of the deposit), and at the base and two lateral boundaries were impervious.

Pore water pressure model in FLIP uses the concept of liquefaction front, in which the state variable S (conceptually equivalent to a mean effective stress) is defined by the combination of liquefaction front parameter, S0, which is a function of the shear work, and shear stress ratio, *r* (Fig. 4). Then modulus is adjusted by a function of mean effective stress ratio. Details on modeling can be found in Iai et al. (1992).

Modeling parameters are defined in Table 2 and 3. They were determined by the standard procedure used in FLIP, i.e., assuming corrected SPT blow count, N65, to be 1 for loose deposit, and 40 for dense deposit. These values of N65 for the deposit of 30 % and 70 % of relative density were determined by engineering judgments and they are confirmed to be within a range of the existing correlations [e.g. Skempton (1986)].

4. Measured and computed deformation of the embankment

Measured and computed deformation of the embankment for four cases (Case 2, 3, 5, and 6) are depicted in Fig. 5. Deformation of Case 1 and 4 were small and not presented. In Fig. 5, upper 50 mm of cross sections of experiments were delineated from photographs taken after shaking. Lower 50 mm were hidden behind the wall of container. Time histories of (a) crest acceleration (A1), (b) crest settlement (D1), and (c) pore water pressure (P2), for Case 3 and 6 are shown in Fig. 6.

At the peak amplitude of input motion 179 Gal for Case 2 in Fig. 5(a), the embankment settled but kept its shape in both measured and computed. Soils near toes are laterally pushed in the direction opposite to the embankment and slightly uplifted, while soils under the embankment were compressed vertically and sheared. The measured amount of crest settlement was 1 m, while it was 0.89 m in the analysis.

At the peak amplitude of 313 Gal for Case 3 in Fig. 5(b), the embankment was laterally expanded and compared to that of Case 2 its shoulders became rounded in the experiment. The large deformation also occurred in the simulation and the deformed shape of the embankment was similar to the experimental counterpart. As shown in Fig. 6(b), LDT reading was saturated due to large settlements, therefore the amount of residual crest settlement was alternatively obtained from the direct measurement of the height of the embankment before and after shaking. Measured and computed residual crest settlements were coincidentally or precisely 1.4 m (47 % of its original height). Although first few cycles of computed crest acceleration shown in Fig. 6(a) are over estimated, the amplitude after five seconds agrees well. Time histories of computed settlements (up to 8 seconds) and pore water pressure buildup shown in Fig. 6(b) and (c) are also consistent with measured ones.

At the peak amplitude of 169 Gal for Case 5 in Fig. 5(c), residual crest settlement was as small as 4.8 mm (0.16 % of its original height) in the experiment and that was 1.3 mm (0.04 %) in the analysis. As shown in Fig. 5(c),

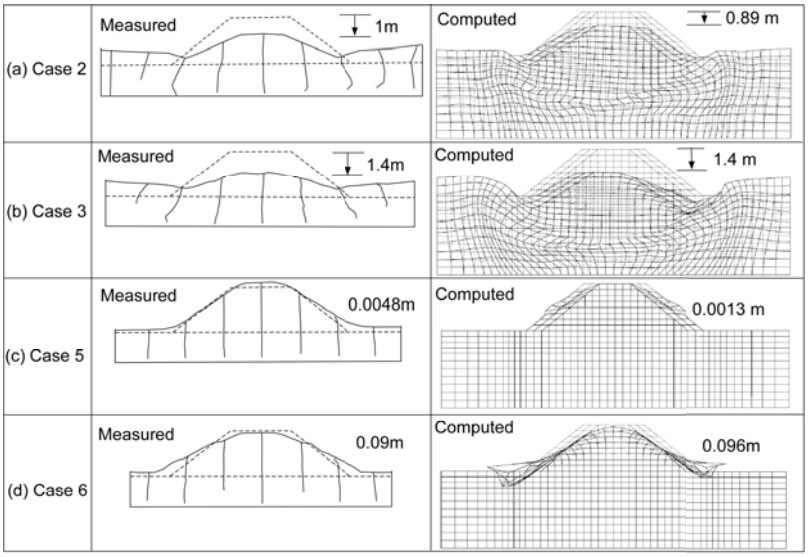

Fig. 5. Measured and computed deformation of the levee: (a) Case 2, (b) Case 3, (c) Case5, and (d) Case 6. Amount of crest settlements are indicated.

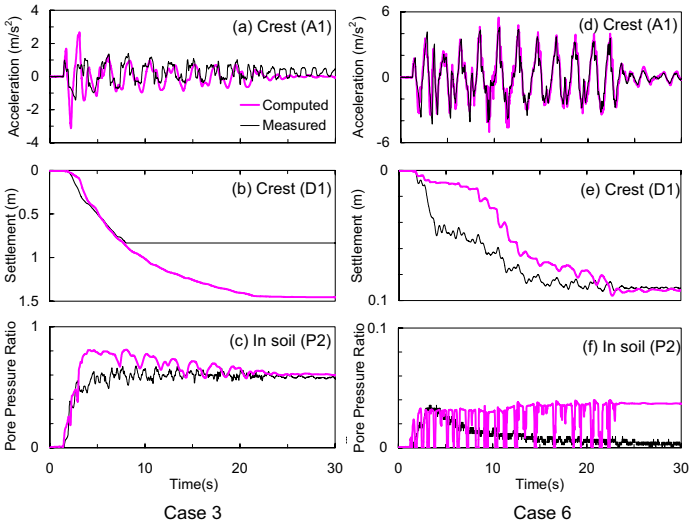

Fig. 6. Time histories of (a) acceleration at the crest (A1), (b) settlement at the crest (D1), (c) pore water pressure buildup (P2) for Case 3, (d) acceleration at the crest (A1), (e) settlement at the crest (D1), and (f) pore water pressure buildup (P2) for Case 6.

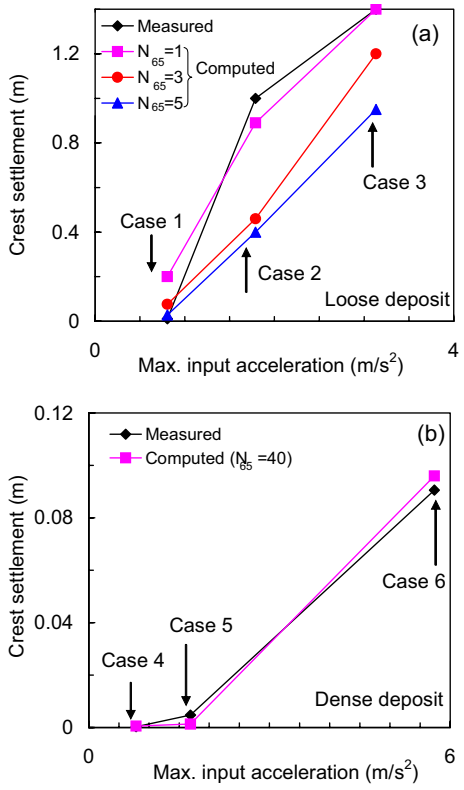

Fig. 7. Variation of settlements versus maximum input acceleration.

shoulders of the embankment were slightly deformed in the analysis, while they are not clearly seen in the measured one. In the experiment, the height of the crown is drawn above the initial level in Fig. 5(c). This might be attributed to primarily model construction error. The photograph taken "before" shaking revealed somehow rounded shape of shoulders, and compared to the photograph after shaking, settlements were hardly detected by the naked eye.

At the peak amplitude of 574 Gal for Case 6 in Fig. 5(d), no deformation was observed in the saturated sand deposit in both computed and measured. Shoulders were rounded in the experiment and some sands were fallen off. Because there was no reduction of input acceleration due to liquefaction, large acceleration was input and shear stress was concentrated at the shoulders in the body of embankment. This may be simulated, however, as shown in Fig. 5(d), mesh is overlapped at the bottom of the embankment. This is because the numerical method used here is based on the assumption of infinitesimal strains, and does not properly simulate large deformations, such as falling off sands.

5. Amounts of settlements and the intensity of shaking

As it is expected, the amount of crest settlements shown in Fig. 7 is proportional to the peak input acceleration in both loose and dense deposit. In Fig. 7(a), three computational results, i.e., model parameters corresponding to N65 of 1, 3 and 5, are shown for comparison purposes together with measured ones. Among these computations, settlements for the case of N65 = 1 are in reasonable agreement with experimental counterpart.

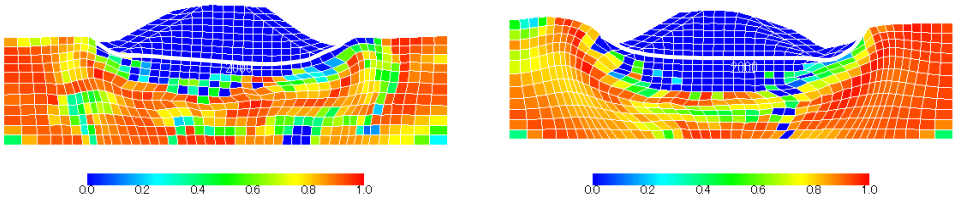

(a) Case 2: at 20 sec (b) Case 3: at 20 sec

Fig 8. Comparison of deformation and pore pressure ratio at 20 sec: (a) Case 2, (b) Case 3. Areas of non-liquefied zone below the levee is larger in Case 3.

Crest settlements on loose deposit were resulted from the deformation of an embankment associated with the settlement of the underneath deposit, while on the dense deposit they were resulted from the deformation of the embankment's body itself (see Fig. 5).

In the analysis for loose deposit, when the input acceleration increased (Case 2 and 3 in Fig. 7), non-liquefied area under the embankment becomes large, leading larger non-liquefied wedge penetrating in a liquefied deposit, i.e., a wedge is pushing more liquefied soils aside. The mechanism can be explained as follows; it is obvious that the mean effective stress just under an embankment is high due to the overburden pressure. However, rocking-like motion of an embankment induced by cyclic input motions may further increase the mean effective stress in the deposit near an embankment, or, equivalently, the area of low pore pressure ratio may be increased by shaking as shown in Fig. 8(b). Although the area shifts left and right with shaking, pore pressure ratio near the center of an embankment is always low, and this arcuate area may become large with the intensity of input motion.

6. Conclusions

Centrifuge experiments under 50 G were conducted to study dynamic behavior of a embankment (3 m height) made of dry sand underlain by saturated sand deposit with 5 m depth. The relative density of saturated sand deposit was approximately either 30 % or 70 %. Conclusions are as follows:

1. It was observed in the centrifuge experiments that the crest settlements and the peak input acceleration was correlated. The numerical method simulated well not only the above-mentioned relation, but also the transient motions, i.e., deformation, acceleration, and pore water pressure buildup, of an embankment on saturated sand deposit during strong shaking, and, therefore, its applicability was confirmed.
2. It was found that, in the analysis for loose deposit, when the input acceleration increased, non-liquefied area underneath the embankment became large, leading larger non-liquefied wedge penetrating in a liquefied deposit i.e., a wedge is pushing more liquefied soils aside. This mechanism may explain why the compacted area underneath an embankment is an effective measure for deformation due to liquefaction. Further experimental studies are needed to verify the wedge formation and to explain mechanism of settlements related to the peak input acceleration.

The relation between the crest settlements and the peak input acceleration obtained from the centrifuge experiments were used only for comparison purposes in the present paper.

Acknowledgements

This study was financially supported by the Ports and Airports Department, Kinki Regional Development Bureau, Ministry of Land, Infrastructure and Transport, Japan, and partially supported by the Ministry of Education, Science, Sports and Culture, Grant-in-Aid for young scientists (B), "Research on the seismic resistance on raised bed river (16710131)", 2004-2005.

References

Adalier, K., Elgamal, A.-W., and Martin, G., M. (1998): Foundation liquefaction countermeasures for earth embankments, Journal of Geotechnical and Environmental Engineering, ASCE, Vol. 124, No. 6, 500-517.

Adalier, K., and Sharp, M., K. (2004): Embankment dam on liquefiable foundation - dynamic behavior and densification remediation, Journal of Geotechnical and Environmental Engineering, Vol. 130, No. 11,

1214-1224.

Bardet, J. P., and Davis, C. A. (1996): Performance of San Fernando dams during the 1994 Northridge Earthquake, Journal of Geotechnical Engineering, ASCE, 122(7), 554-564.

Fiegel, G., L., and Kutter, B., L. (1994): Liquefaction-induced lateral spreading of mildly sloping ground, Journal of Geotechnical Engineering, ASCE, 120(8), 2236-2243.

Finn, W. D. L. (2000): State-of-the-art of geotechnical earthquake engineering practice, Soil Dynamics and Earthquake Engineering, Vol. 20, No. 1, 1-15.

GHQ-Report. (1948): The Fukui Earthqauke, Hokuriku Region, Japan 28 June 1948, General Headquarters, Far East Command, Gendai Shiryo Shuppan, 1998, Tokyo.

Iai, S., Matsunaga, Y., and Kameoka, T. (1992): Strain space plasticity model for cyclic mobility, Soils and Foundations, Japanese Society of Soil Mechanics and Foundation Engineering, Vol. 32, No. 2, 1- 15.

ISO23469. (2005): Bases for design of structures - Seismic actions for designing geotechnical works, International Organization of Standardization.

Kazama, M., Inatomi, T., Iizuka, E., and Nagayoshi, T. (1996): Stability of embankment on liquefiable sand layers in centrifuge shaking table tests, Journal of Geotechnical Engineering, JSCE, 547/III-36, 107-106 (in Japanese).

Koga, Y., and Matsuo, O. (1990): Shaking table tests of embankments rsting on liquefiable sandy ground, Soils and Foundations, Vol. 30, No. 4, 162-174.

Koseki, J., Koga, Y., and Takahashi, A. (1994): Liquefaction of sandy ground and settlement of embankments, Proc. of Centrifuge 94, 215-220.

Matsuo, O. (1996): Damage to river dikes, Special Issue of Soils and Foundations, Japanese Geotechnical Society, 235-240.

Microsoft. (2003): Windows XP Professional, Microsoft Co., One Microsoft Way, Redmond, WA 98052-6399, USA."

Nishimoto, S. (2003): Damage on levees, Recconaissance report on the 2003 Tokachi-oki, Japan, Earthquake, JSCE (in Japanese), http://www.jsce.or.jp/.

Seed, H. B., Lee, K. L., Idriss, I. M., and Makdisi, F. I. (1975): The slides in the San Fernando Dams during the earthquake of February 9, 1971, Journal of Geotechnical Engineering, ASCE, Vol. 101, No. 7, 651-688.

Seed, R. B., Dickenson, S. E., Riemer, M. F., Bray, J. D., Sitar, N., Mitchell, J. K., Idriss, I. M., Kayen, R. E., Kropp, A., Hander, L. F. J., and Power, M. S. (1990): Preliminary Report on the Principal Geotechnical Aspects of the October 17, 1989, Loma Prieta Earthquake, Report No. UCB/EERC-90/05, Earthquake Engineering Research Center, University of California Berkeley.

Skempton, A. W. (1986): Standard penetration test procedures and the effects in sands of overburden pressure, relative density, particle size, ageing and overconsolidation, Geotechnique, 36(3), 425-447.

Takeuchi, M., Yanagihara, S., and Ishihara, K. (1991): Shaking table tests on model dikes founded on sand deposits with compacted zone, Proceedings of International Conference on Geotechnical Engineering for Coastal Development (GEO-COAST'91), Yokohama, Japan, 2 Vols., 1, 509-514.

Yasuda, S., Yoshida, N., Adachi, K., Kiku, H., and Gose, S. (1999): A simplified analysis of liquefaction-induced residual deformation, Proceedings of the 2nd Internatinal Conference on Earthquake Geotechnical Engineering, 555-560.

飽和砂地盤上の盛土の動的変形挙動

飛田哲男・井合進・上田恭平*

*京都大学工学研究科社会基盤工学専攻

要旨

飽和砂地盤上の盛土の動的変形挙動を調べるため，遠心模型実験，および多重せん断ばねモデルによる有限要素解析（FLIP）を行った．本研究で対象とした盛土は，堤体高さ3m，天端と下端の長さが4mと11.5m（実物スケール）である．また下部地盤の層厚は5mである．緩詰地盤を対象とした数値解析では地盤のN値=１に対応するパラメータを用いた場合に，天端の沈下量が実験結果と良く一致した．数値解析の結果，入力加速度が大きいほど，盛土下部の非液状化領域が大きくなり，それがくさびとなって周辺の液状化地盤を押しのけるため沈下量が大きくなるという，一見すると直感的ではない変形メカニズムが推察された．

キーワード:盛土，地震時挙動，液状化，遠心模型実験，数値解析